

Molecular pentaquarks composed of a ground octet baryon and a P -wave anti-charmed meson

Yu-Yue Cui¹, Rui Chen^{1,2,*} and Qi Huang³

¹Key Laboratory of Low-Dimensional Quantum Structures and Quantum Control of Ministry of Education, Department of Physics and Synergetic Innovation Center for Quantum Effects and Applications, Hunan Normal University, Changsha 410081, China

²Hunan Research Center of the Basic Discipline for Quantum Effects and Quantum Technologies, Hunan Normal University, Changsha 410081, China

³School of Physics and Technology, Nanjing Normal University, Nanjing 210023, China

(Dated: January 21, 2026)

In this work, we investigate the interactions between an excited anti-charm meson doublet (\bar{D}_1, \bar{D}_2^*) and ground-state octet baryons (N, Λ, Σ, Ξ) with the aim of identifying possible molecular pentaquark states. A systematic analysis is performed within the one-boson-exchange model, which incorporates both S -wave and P -wave interactions, S - D wave mixing, and coupled-channel effects. By solving the Schrödinger equations, we can predict a rich spectrum of loosely bound anti-charm molecular pentaquarks with strangeness $|S| = 0, 1, 2$. Our results provide specific quantum number assignments and mass range predictions to guide future experimental searches at facilities such as LHCb and Belle II. The discovery of such states would significantly enrich the hadron spectrum and serve as a critical test of theoretical models for hadronic interactions.

PACS numbers: 12.39.Pn, 14.20.Pt, 14.40.Lb, 14.20.Jn

I. INTRODUCTION

The search for exotic states—hadrons beyond the conventional quark-antiquark mesons and three-quark baryons—has been a central pursuit in hadron physics since the quark model was proposed [1–3]. These exotic structures serve as unique laboratories for probing quantum chromodynamics (QCD) in the strongly coupled, non-perturbative regime, advancing our fundamental understanding of matter and interaction.

Among these particles, pentaquark states, comprising four quarks and one antiquark, constitute an important and intriguing category of exotic hadrons. Theoretical investigations on their existence can be traced back to 1979, when Strottman calculated the masses of light-quark pentaquarks within the MIT bag model [4]. Then, studies that explored the possibilities of stable pentaquarks containing a charm quark was carried out [5, 6]. The first tentative experimental evidence emerged in 2003 with the LEPs Collaboration’s report of the $\Theta(1530)$, a state interpreted as a pentaquark composed of four light quarks and an \bar{s} antiquark [7]. However, subsequent high-statistics experiments failed to confirm this observation [8]. Similarly, early evidence for other candidates, such as the double-strange $\Xi^-(dds\bar{s})$ [9] and the anti-charmed $\Theta_c(uudd\bar{c})$ [10], could not be independently verified [11–13].

However, things changed dramatically in the past decade. In 2015, the LHCb Collaboration announced the discovery of two hidden-charm pentaquarks, $P_c(4380)$ and $P_c(4450)$, in the decay $\Lambda_b^0 \rightarrow J/\psi p K^-$ [14]. A subsequent analysis with combined Run I and Run II data in 2019 not only revealed a new narrow state, $P_c(4312)$, but also resolved the $P_c(4450)$ into two distinct peaks, $P_c(4440)$ and $P_c(4457)$ [15].

The proximity of these states to the $\Sigma_c \bar{D}^{(*)}$ thresholds has led to a widespread molecular interpretation in theoretical

studies [16–44]. In our previous work, we employed the one-boson-exchange (OBE) model to study the interactions between a charmed baryon and an anti-charmed meson. Our results supported the identification of $P_c(4312)$, $P_c(4440)$, and $P_c(4457)$ as $\Sigma_c \bar{D}$, $\Sigma_c \bar{D}^*$, and $\Sigma_c \bar{D}^*$ molecules with $I(J^P) = 1/2(1/2^-)$, $1/2(1/2^-)$, and $1/2(3/2^-)$, respectively, and highlighted the importance of coupled-channel effects [21]. It is worth noting that theoretical predictions for such hidden-charm molecular baryons existed prior to their experimental discovery [45–50].

Obviously, with the ongoing accumulation of experimental data and advances in technique, discoveries on additional pentaquark states must be possible. Thus, it is both timely and important to carry out theoretical investigations on other possible molecular pentaquark configurations. Such studies can not only enrich the hadron spectrum, but also provide a deeper understanding of strong interactions in the non-perturbative region, and offer further insights into the molecular nature of the observed exotic states.

In this work, we investigate the interactions between an anti-charmed meson $\bar{T} = (\bar{D}_1, \bar{D}_2^*)$ and an octet baryon $B = (N, \Lambda, \Sigma, \Xi)$ to predict possible $\bar{T}B$ molecular pentaquarks. Compared to the well-studied $\Sigma_c \bar{D}^{(*)}$ systems, the $\bar{T}B$ configurations present distinct characteristics. On the one hand, the larger number of light quarks in the $\bar{T}B$ systems may enhance the contributions from light meson exchange. On the other hand, the relatively smaller reduced mass of these systems results in a larger kinetic energy, which can suppress bound-state formation. Thus, these two opposite traits make such a kind of system interesting and meaningful to be investigated, which can at least help us seek the boundary of interaction through experimental verification.

Our exploration builds upon earlier work, where we predicted possible molecular pentaquarks composed of $D_1 N$ and $D_2^* N$ using an effective potential based on one-pion exchange [51]. The $\bar{T}B$ systems offer a simpler theoretical framework than their TB counterparts, as they avoid complications aris-

*Electronic address: chenrui@hunnu.edu.cn

ing from quark annihilation processes. In the present study, we employ a comprehensive OBE model to derive the effective potentials, which means apart from the long-range OPE contribution, we also include intermediate- and short-range interactions mediated by scalar (σ) and vector (ρ , ω) meson exchanges. In addition, we consider the coupled-channel effects, which were previously shown to be crucial for generating D_1N and D_2^*N molecular candidates [51]. The coupled-channel Schrödinger equation is then solved to search for loosely bound molecular states.

This paper is organized as follows. In Sec. II, we derive the OBE effective potentials for the systems under study. The numerical results are presented and discussed in Sec. III. Finally, a summary is provided in Sec. IV.

II. THE OBE INTERACTIONS

We begin with the constructions on the flavor and spin-orbit wave functions, which are summarized in Table I. The general forms of the spin-orbit wave functions are

$$|\bar{D}_1 B(2S+1L_J)\rangle = \sum_{m,m',m_S m_L} C_{\frac{1}{2}m,1m'}^{S,m_S} C_{S m_S, L m_L}^{J,M} \chi_{\frac{1}{2}m} \epsilon^{m'} |Y_{L,m_L}\rangle,$$

$$|\bar{D}_2^* B(2S+1L_J)\rangle = \sum_{m,m',m_S m_L} C_{\frac{1}{2}m,2m'}^{S,m_S} C_{S m_S, L m_L}^{J,M} \chi_{\frac{1}{2}m} \zeta^{m'} |Y_{L,m_L}\rangle,$$

where $C_{j_1 m_1, j_2 m_2}^{J,M}$ are Clebsch-Gordan coefficients. Here, $\chi_{\frac{1}{2}m}$ and Y_{L,m_L} denote the spinor of the ground-state baryon and the spherical harmonic function, respectively. The polarization vector for the \bar{D}_1 meson is ϵ_m^μ ($m = 0, \pm 1$), and the polarization tensor for the \bar{D}_2^* meson is constructed as $\zeta_m^{\mu\nu} = \sum_{m_1, m_2} \langle 1, m_1; 1, m_2 | 2, m \rangle \epsilon_{m_1}^\mu \epsilon_{m_2}^\nu$ [52], with the explicit representations $\epsilon_\pm^\mu = (0, \pm 1, i, 0)/\sqrt{2}$ and $\epsilon_0^\mu = (0, 0, 0, -1)$.

The OBE effective potentials are derived through the following standard procedure. After constructing the relevant effective Lagrangians, we obtain the scattering amplitudes $\mathcal{M}(\bar{T}_i B_i \rightarrow \bar{T}_f B_f)$ for t -channel single-meson (M) exchange. The momentum-space potential in the nonrelativistic limit is then given by the Breit approximation as

$$\mathcal{V}_M^{\bar{T}_i B_i \rightarrow \bar{T}_f B_f}(q) = -\frac{\mathcal{M}(\bar{T}_i B_i \rightarrow \bar{T}_f B_f)}{\sqrt{2m_{\bar{T}_i} 2m_{B_i} 2m_{\bar{T}_f} 2m_{B_f}}}. \quad (1)$$

The contributing mesons M are the scalar σ , pseudoscalars π and η , and vectors ρ and ω . The coordinate-space potential $\mathcal{V}(r)$ follows from the Fourier transform as

$$\mathcal{V}(r) = \int \frac{d^3\vec{q}}{(2\pi)^3} e^{i\vec{q}\cdot\vec{r}} \mathcal{V}(q) \mathcal{F}^2(q^2, m_E^2). \quad (2)$$

Here, a monopole form factor $\mathcal{F}(q^2, m_E^2) = (\Lambda^2 - m_E^2)/(\Lambda^2 - q^2)$ is introduced at each vertex to account for the composite nature of the hadrons and to regulate the high-momentum divergence, where Λ , m_E , and q are the cutoff parameter, mass, and four-momentum of the exchanged meson, respectively. Based on the successful description of the deuteron and other molecular candidates [21–25, 46, 47, 53–85], we vary Λ in a reasonable range around 1.00 GeV.

TABLE I: The flavor wave functions $|I, I_3\rangle$ and spin-orbit wave functions $|^{2S+1}L_J\rangle$ for the discussed $\bar{T}B$ systems.

$ I, I_3\rangle$	$J^P ^{2S+1}L_J\rangle$
$\bar{T}N$ $ 1, 1\rangle = \bar{T}^0 p$	$\bar{D}_1 B$ $\frac{1}{2}^+$ $ ^2S_{\frac{1}{2}}, ^4D_{\frac{1}{2}}\rangle$
$ 1, 0\rangle = \frac{1}{\sqrt{2}}(\bar{T}^0 n + T^- p)$	$\frac{3}{2}^+$ $ ^4S_{\frac{3}{2}}, ^2D_{\frac{3}{2}}, ^4D_{\frac{3}{2}}\rangle$
$ 1, -1\rangle = T^- n$	$\frac{1}{2}^-$ $ ^2P_{\frac{1}{2}}, ^4P_{\frac{1}{2}}\rangle$
$ 0, 0\rangle = \frac{1}{\sqrt{2}}(\bar{T}^0 n - T^- p)$	$\frac{3}{2}^-$ $ ^2P_{\frac{3}{2}}, ^4P_{\frac{3}{2}}\rangle$
$\bar{T}\Lambda$ $ \frac{1}{2}, \frac{1}{2}\rangle = \bar{T}^0 \Lambda^0$	$\frac{5}{2}^-$ $ ^4P_{\frac{5}{2}}\rangle$
$ \frac{1}{2}, -\frac{1}{2}\rangle = T^- \Lambda^0$	$\bar{D}_2^* B$ $\frac{1}{2}^+$ $ ^4D_{\frac{1}{2}}, ^6D_{\frac{1}{2}}\rangle$
$\bar{T}\Sigma$ $ \frac{1}{2}, \frac{1}{2}\rangle = \sqrt{\frac{1}{3}}\bar{T}^0 \Sigma^0 - \sqrt{\frac{2}{3}}T^- \Sigma^+$	$\frac{3}{2}^+$ $ ^4S_{\frac{3}{2}}, ^4D_{\frac{3}{2}}, ^6D_{\frac{3}{2}}\rangle$
$ \frac{1}{2}, -\frac{1}{2}\rangle = -\sqrt{\frac{1}{3}}T^- \Sigma^0 + \sqrt{\frac{2}{3}}\bar{T}^0 \Sigma^-$	$\frac{5}{2}^+$ $ ^6S_{\frac{5}{2}}, ^4D_{\frac{5}{2}}, ^6D_{\frac{5}{2}}\rangle$
$ \frac{3}{2}, \frac{3}{2}\rangle = \bar{T}^0 \Sigma^+$	$\frac{1}{2}^-$ $ ^4P_{\frac{1}{2}}\rangle$
$ \frac{3}{2}, \frac{1}{2}\rangle = \sqrt{\frac{2}{3}}\bar{T}^0 \Sigma^0 + \sqrt{\frac{1}{3}}T^- \Sigma^+$	$\frac{3}{2}^-$ $ ^4P_{\frac{3}{2}}, ^6P_{\frac{3}{2}}\rangle$
$ \frac{3}{2}, -\frac{1}{2}\rangle = \sqrt{\frac{2}{3}}T^- \Sigma^0 + \sqrt{\frac{1}{3}}\bar{T}^0 \Sigma^-$	$\frac{5}{2}^-$ $ ^4P_{\frac{5}{2}}, ^6P_{\frac{5}{2}}\rangle$
$ \frac{3}{2}, -\frac{3}{2}\rangle = T^- \Sigma^-$	$\frac{7}{2}^-$ $ ^6P_{\frac{7}{2}}\rangle$
$\bar{T}\Xi$ $ 1, 1\rangle = \bar{T}^0 \Xi^0$	
$ 1, 0\rangle = \frac{1}{\sqrt{2}}(\bar{T}^0 \Xi^- + T^- \Xi^0)$	
$ 1, -1\rangle = T^- \Xi^-$	
$ 0, 0\rangle = \frac{1}{\sqrt{2}}(\bar{T}^0 n - T^- p)$	

The effective Lagrangians governing the interactions of the P -wave anti-charmed meson doublet (\bar{D}_1, \bar{D}_2^*) with light mesons are constructed with heavy quark symmetry and chiral symmetry [86–89] as follows

$$\mathcal{L} = g_\sigma' \langle \bar{T}_b^{(\bar{Q})\mu} \sigma T_{b\mu}^{(Q)} \rangle + ik \langle \bar{T}_a^{(\bar{Q})\mu} \mathcal{A}_{ab} \gamma_5 T_{b\mu}^{(Q)} \rangle - \langle i \bar{T}_{a\lambda}^{(\bar{Q})} (\beta'' v^\mu (\mathcal{V}_\mu - \rho_\mu) - \lambda'' \sigma^{\mu\nu} F_{\mu\nu}(\rho))_{ab} T_b^{(Q)\lambda} \rangle, \quad (3)$$

where the axial current $\mathcal{A}_\mu = \frac{1}{2}(\xi^\dagger \partial_\mu \xi - \xi \partial_\mu \xi^\dagger)_\mu$, vector current $\mathcal{V}_\mu = \frac{1}{2}(\xi^\dagger \partial_\mu \xi + \xi \partial_\mu \xi^\dagger)_\mu$, and vector meson field strength $F_{\mu\nu}(\rho) = \partial_\mu \rho_\nu - \partial_\nu \rho_\mu + [\rho_\mu, \rho_\nu]$ are defined in the standard chiral perturbation theory formalism. The pseudo-Goldstone and vector meson matrices are $\xi = \exp(i\mathbb{P}/f_\pi)$ and $\rho_\mu = ig_V \mathbb{V}_\mu / \sqrt{2}$, respectively. The superfield $T^{(Q)\mu} a$, which combines the \bar{D}_1 and \bar{D}_2^* states, is

$$T_a^{(\bar{Q})\mu} = \left[\bar{D}_{2a}^{*(\bar{Q})\mu\nu} \gamma_\nu - \sqrt{\frac{3}{2}} \bar{D}_{1a\nu}^{(\bar{Q})} \gamma_5 \left(g^{\mu\nu} - \frac{1}{3}(\gamma^\mu - v^\mu) \gamma^\nu \right) \right] \mathcal{P}_-$$

Here, $\mathcal{P}_- = (1 - \not{v})/2$ is the heavy quark projection operator, and $v^\mu = (1, 0, 0, 0)$ is the four-velocity of heavy quark in the non-relativistic approximation.

After expanding Eq. (3), we further obtain the explicit interaction Lagrangians as

$$\mathcal{L}_{\bar{D}_1 \bar{D}_1 \sigma} = -2g_\sigma'' \bar{D}_{1a\mu} \bar{D}_{1a}^{\mu\dagger} \sigma, \quad (4)$$

$$\mathcal{L}_{\bar{D}_2^* \bar{D}_2^* \sigma} = 2g_\sigma'' \bar{D}_{2a\mu\nu}^{*\dagger} \bar{D}_{2a}^{*\mu\nu} \sigma, \quad (5)$$

$$\mathcal{L}_{\bar{D}_1 \bar{D}_2^* \sigma} = \sqrt{\frac{2}{3}} i g_\sigma'' \epsilon^{\mu\nu\rho\tau} v_\rho (\bar{D}_{1a\nu}^\dagger \bar{D}_{2a\mu\tau}^* - \bar{D}_{1a\nu} \bar{D}_{2a\mu\tau}^{*\dagger}) \sigma, \quad (6)$$

$$\mathcal{L}_{\bar{D}_1 \bar{D}_1 \mathbb{P}} = -\frac{5ik}{3f_\pi} \epsilon^{\mu\nu\rho\tau} v_\nu \bar{D}_{1a\rho}^\dagger \bar{D}_{1b\tau} \partial_\mu \mathbb{P}_{ab}, \quad (7)$$

$$\mathcal{L}_{\bar{D}_2^* \bar{D}_2^* \mathbb{P}} = \frac{2ik}{f_\pi} \epsilon^{\mu\nu\rho\tau} v_\nu \bar{D}_{2a\rho}^{*\dagger} \bar{D}_{2b\alpha\tau}^* \partial_\mu \mathbb{P}_{ab}, \quad (8)$$

$$\mathcal{L}_{\bar{D}_1 \bar{D}_2^* \mathbb{P}} = \sqrt{\frac{2}{3}} \frac{k}{f_\pi} (\bar{D}_{2a}^{*\mu\lambda} \bar{D}_{1b\mu}^\dagger + \bar{D}_{1a\mu} \bar{D}_{2b}^{*\mu\lambda\dagger}) \partial_\lambda \mathbb{P}_{ab}, \quad (9)$$

$$\begin{aligned} \mathcal{L}_{\bar{D}_1 \bar{D}_1 \mathbb{V}} &= \sqrt{2} \beta'' g_V (v \cdot \mathbb{V}_{ab}) \bar{D}_{1a\mu} \bar{D}_{1b}^{\mu\dagger} \\ &+ \frac{5\sqrt{2}i\lambda'' g_V}{3} (\bar{D}_{1a}^\nu \bar{D}_{1b}^{\mu\dagger} - \bar{D}_{1a}^{\nu\dagger} \bar{D}_{1b}^\mu) \partial_\mu \mathbb{V}_{abv}, \end{aligned} \quad (10)$$

$$\begin{aligned} \mathcal{L}_{\bar{D}_2^* \bar{D}_2^* \mathbb{V}} &= -\sqrt{2} \beta'' g_V (v \cdot \mathbb{V}_{ab}) \bar{D}_{2a}^{*\nu\lambda} \bar{D}_{2b}^{*\mu\dagger} + 2\sqrt{2}i\lambda'' g_V \\ &\times (\bar{D}_{2a}^{*\lambda\nu\dagger} \bar{D}_{2b}^{*\mu} - \bar{D}_{2a}^{*\lambda\nu} \bar{D}_{2b}^{*\mu\dagger}) \partial_\mu \mathbb{V}_{abv}, \end{aligned} \quad (11)$$

$$\begin{aligned} \mathcal{L}_{\bar{D}_1 \bar{D}_2^* \mathbb{V}} &= \frac{i\beta'' g_V}{\sqrt{3}} \epsilon^{\lambda\rho\tau} v_\rho (\bar{D}_{1a\alpha}^\dagger \bar{D}_{2b\lambda\tau}^* - \bar{D}_{1a\alpha} \bar{D}_{2b\lambda\tau}^{*\dagger}) \\ &+ \frac{2\lambda'' g_V}{\sqrt{3}} [3\epsilon^{\mu\lambda\nu\tau} v_\lambda (\bar{D}_{1a}^{\alpha\dagger} \bar{D}_{2b\alpha\tau}^* + \bar{D}_{1a}^\alpha \bar{D}_{2b\alpha\tau}^{*\dagger}) \partial_\mu \mathbb{V}_{abv} \\ &+ 2\epsilon^{\lambda\rho\nu} v_\rho (\bar{D}_{1a\alpha}^\dagger \bar{D}_{2b\lambda}^{*\mu} + \bar{D}_{1a\alpha} \bar{D}_{2b\lambda}^{\mu\dagger}) \\ &\times (\partial_\mu \mathbb{V}_{abv} - \partial_\nu \mathbb{V}_{ab\mu})]. \end{aligned} \quad (12)$$

As for the interactions between the light octet baryons (B) and light mesons, we employ the following $SU(3)$ -symmetric Lagrangians as

$$\mathcal{L}_{BB\sigma} = g_{BB\sigma} \bar{B} \sigma B, \quad (13)$$

$$\mathcal{L}_{BB\mathbb{P}} = \sqrt{2} \frac{g_{BB\mathbb{P}}}{m_P} \bar{B} \gamma^5 \gamma^\mu \partial_\mu \mathbb{P}_{ba} B, \quad (14)$$

$$\mathcal{L}_{BB\mathbb{V}} = \sqrt{2} g_{BB\mathbb{V}} \bar{B} \gamma^\mu \mathbb{V}_{ba\mu} B - \frac{f_{BB\mathbb{V}}}{\sqrt{2}m_B} \bar{B} \sigma^{\mu\nu} \partial_\nu \mathbb{V}_{ba\mu} B, \quad (15)$$

where pseudoscalar meson matrices \mathbb{P} and vector meson matrices \mathbb{V}_μ are expressed as

$$\begin{aligned} \mathbb{P} &= \begin{pmatrix} \frac{\pi^0}{\sqrt{2}} + \frac{\eta}{\sqrt{6}} & \pi^+ & K^+ \\ \pi^- & -\frac{\pi^0}{\sqrt{2}} + \frac{\eta}{\sqrt{6}} & K^0 \\ K^- & \bar{K}^0 & -\sqrt{\frac{2}{3}}\eta \end{pmatrix}, \\ \mathbb{V}_\mu &= \begin{pmatrix} \frac{\rho^0}{\sqrt{2}} + \frac{\omega}{\sqrt{2}} & \rho^+ & K^{*+} \\ \rho^- & -\frac{\rho^0}{\sqrt{2}} + \frac{\omega}{\sqrt{2}} & K^{*0} \\ K^{*-} & \bar{K}^{*0} & \phi \end{pmatrix}_\mu, \\ B &= \begin{pmatrix} \frac{\Sigma^0}{\sqrt{2}} + \frac{\Lambda}{\sqrt{6}} & \Sigma^+ & p \\ \Sigma^- & -\frac{\Sigma^0}{\sqrt{2}} + \frac{\Lambda}{\sqrt{6}} & n \\ \Xi^- & \Xi^0 & -\frac{2}{\sqrt{6}}\Lambda \end{pmatrix}. \end{aligned}$$

respectively. Then, for all the coupling constants, they are estimated from well-established nucleon-nucleon interactions

TABLE II: Coupling constants adopted in our calculations.

$\frac{g_{\sigma NN}^2}{4\pi} = 5.69$	$g_{NN\eta} = 0.33$	$\frac{g_{\pi NN}^2}{4\pi} = 0.07$	$g_{\Lambda\Lambda\omega} = 7.98$
$\frac{g_{\rho NN}^2}{4\pi} = 0.81$	$f_{\Lambda\Lambda\omega} = -9.73$	$\frac{f_{\rho NN}}{g_{\rho NN}} = 6.10$	$g_{\Lambda\Lambda\eta} = -0.67$
$\frac{g_{\omega NN}^2}{4\pi} = 20.00$	$\frac{f_{\omega NN}}{g_{\omega NN}} = 0.00$	$k = 0.78$	$f_\pi = 0.13$
$f_{\Lambda\Sigma\rho} = 16.85$	$g_{\Lambda\Sigma\rho} = -0.55$	$g_{\Lambda\Sigma\pi} = 0.67$	$g_{N\Sigma K} = 0.19$
$g_{\Sigma\Sigma\rho/\omega} = 7.34$	$f_{\Sigma\Sigma\rho/\omega} = 9.73$	$g_{\Sigma\Sigma\pi} = 0.77$	$g_{\Sigma\Sigma\eta} = 0.67$
$g_{\Xi\Xi\pi} = -0.19$	$g_{\Xi\Xi\eta} = -0.99$	$g_{\Xi\Xi\rho/\omega} = 4.23$	$\lambda'' g_V = 7.38$
$f_{\Xi\Xi\rho/\omega} = -9.91$	$g_\sigma = 2.82$	$\beta'' g_V = -6.50$	

TABLE III: The isospin factor for different exchanged mesons in our calculations.

	I	\mathcal{G}_σ	\mathcal{G}_π	\mathcal{G}_η	\mathcal{G}_ρ	\mathcal{G}_ω
$\bar{T}N - \bar{T}N$	0	1	$\frac{3}{2}$	$\frac{\sqrt{3}}{6}$	$\frac{3}{2}$	$\frac{1}{2}$
	1	1	$-\frac{1}{2}$	$\frac{\sqrt{3}}{6}$	$-\frac{1}{2}$	$\frac{1}{2}$
$\bar{T}\Lambda - \bar{T}\Lambda$	$\frac{1}{2}$	1	-	$\frac{\sqrt{3}}{6}$	-	$\frac{1}{2}$
$\bar{T}\Sigma - \bar{T}\Sigma$	$\frac{1}{2}$	1	1	$\frac{\sqrt{3}}{6}$	1	$\frac{1}{2}$
	$\frac{3}{2}$	1	$-\frac{1}{2}$	$\frac{\sqrt{3}}{6}$	$-\frac{1}{2}$	$\frac{1}{2}$
$\bar{T}\Xi - \bar{T}\Xi$	0	1	$\frac{3}{2}$	$\frac{1}{2\sqrt{3}}$	$\frac{3}{2}$	$\frac{1}{2}$
	1	1	$-\frac{1}{2}$	$\frac{1}{2\sqrt{3}}$	$-\frac{1}{2}$	$\frac{1}{2}$
$\bar{T}\Lambda - \bar{T}\Sigma$	$\frac{1}{2}$	-	$-\frac{\sqrt{3}}{2}$	-	$-\frac{\sqrt{3}}{2}$	-

through the quark model and $SU(3)$ symmetry relations [48, 90–93], whose numerical values are compiled in Table II.

The total OBE effective potential for a given $\bar{T}B$ channel is a sum over the exchanged mesons M as

$$V_{\bar{T}B} = \sum_M \mathcal{G}_M \mathcal{V}_{\bar{T}B \rightarrow \bar{T}B}^M, \quad (16)$$

where \mathcal{G}_M is the isospin factor listed in Table III. And $\mathcal{V}_{\bar{T}B \rightarrow \bar{T}B}^M$ are the OBE subpotentials for the process $\bar{T}B \rightarrow \bar{T}B$ by exchanging meson M , i.e.,

$$\mathcal{V}_{\bar{D}_1 B \rightarrow \bar{D}_1 B}^\sigma = -C_1 \mathcal{A}_1 Y_{\Lambda, m_\sigma}, \quad (17)$$

$$\mathcal{V}_{\bar{D}_1 B \rightarrow \bar{D}_1 B}^{\pi, \eta} = \frac{5C_2}{9\sqrt{2}} (\mathcal{A}_2 Z_{\Lambda, m_P} + \mathcal{A}_3 T_{\Lambda, m_P}), \quad (18)$$

$$\begin{aligned} \mathcal{V}_{\bar{D}_1 B \rightarrow \bar{D}_1 B}^{\rho, \omega} &= -\frac{5C_3}{9} \mathcal{A}_2 Z_{\Lambda, m_V} + \frac{5C_3}{18} \mathcal{A}_3 T_{\Lambda, m_V} \\ &- C_4 \mathcal{A}_1 Y_{\Lambda, m_V}, \end{aligned} \quad (19)$$

$$\mathcal{V}_{\bar{D}_2^* B \rightarrow \bar{D}_2^* B}^\sigma = -C_1 \mathcal{A}_4 Y_{\Lambda, m_\sigma}, \quad (20)$$

$$\mathcal{V}_{\bar{D}_2^* B \rightarrow \bar{D}_2^* B}^{\pi, \eta} = \frac{\sqrt{2}C_2}{3} (\mathcal{A}_5 Z_{\Lambda, m_P} + \mathcal{A}_6 T_{\Lambda, m_P}), \quad (21)$$

$$\mathcal{V}_{\bar{D}_2^* B \rightarrow \bar{D}_2^* B}^{\rho/\omega} = \frac{C_3}{3} \mathcal{A}_6 T_{\Lambda, m_V} - \frac{2C_3}{3} \mathcal{A}_5 Z_{\Lambda, m_V}$$

TABLE IV: Matrix elements for the spin-spin interactions and tensor force operators in the OBE effective potentials. Here, $\langle \mathcal{A}_1 \rangle = \langle \mathcal{A}_4 \rangle = \mathcal{I}$ with \mathcal{I} being the identity matrix.

J^P	\mathcal{A}_2	\mathcal{A}_3	\mathcal{A}_5	\mathcal{A}_6	\mathcal{A}_7	\mathcal{A}_8
$\frac{1}{2}^-$	$\begin{pmatrix} -2 & 0 \\ 0 & 1 \end{pmatrix}$	$\begin{pmatrix} 0 & -\sqrt{2} \\ -\sqrt{2} & -2 \end{pmatrix}$	$\begin{pmatrix} 0 \\ \sqrt{\frac{5}{2}} \end{pmatrix}$	$\begin{pmatrix} \sqrt{\frac{5}{5}} \\ \sqrt{\frac{2}{5}} \end{pmatrix}$	$\begin{pmatrix} -\frac{3}{2} & 0 \\ 0 & 1 \end{pmatrix}$	$\begin{pmatrix} -\frac{12}{25} & -\frac{63}{50} \\ -\frac{63}{50} & -\frac{28}{25} \end{pmatrix}$
$\frac{3}{2}^-$	$\begin{pmatrix} -2 & 0 \\ 0 & 1 \end{pmatrix}$	$\begin{pmatrix} 0 & \frac{1}{\sqrt{5}} \\ \frac{1}{\sqrt{5}} & \frac{8}{5} \end{pmatrix}$	$\begin{pmatrix} 0 & 0 \\ \sqrt{\frac{5}{2}} & 0 \end{pmatrix}$	$\begin{pmatrix} -\frac{1}{5\sqrt{2}} & -\frac{6\sqrt{2}}{5} \\ -\frac{4}{5}\sqrt{\frac{2}{5}} & -\frac{21}{5\sqrt{10}} \end{pmatrix}$	$\begin{pmatrix} -\frac{3}{2} & 0 \\ 0 & 1 \end{pmatrix}$	$\begin{pmatrix} \frac{3}{25} & \frac{9}{25}\sqrt{\frac{7}{2}} \\ \frac{9}{25}\sqrt{\frac{7}{2}} & \frac{32}{25} \end{pmatrix}$
$\frac{5}{2}^-$	(-1)	(0)	$(0 \ \sqrt{\frac{5}{2}})$	$(\frac{1}{5}\sqrt{\frac{2}{5}} \ \frac{3}{5}\sqrt{\frac{7}{5}})$	(0)	$(\frac{3}{5})$
$\frac{1}{2}^+$	$\begin{pmatrix} -2 & 0 \\ 0 & 1 \end{pmatrix}$	$\begin{pmatrix} 0 & -\sqrt{2} \\ -\sqrt{2} & -2 \end{pmatrix}$	$\begin{pmatrix} 0 & 0 \\ \sqrt{\frac{5}{2}} & 0 \end{pmatrix}$	$\begin{pmatrix} \frac{1}{\sqrt{5}} & 2\sqrt{\frac{6}{5}} \\ \sqrt{\frac{2}{5}} & -\sqrt{\frac{3}{5}} \end{pmatrix}$	$\begin{pmatrix} -\frac{3}{2} & 0 \\ 0 & 1 \end{pmatrix}$	$\begin{pmatrix} \frac{3}{5} & -\frac{3}{5}\sqrt{\frac{3}{2}} \\ -\frac{3}{5}\sqrt{\frac{3}{2}} & -\frac{8}{5} \end{pmatrix}$
$\frac{3}{2}^+$	$\begin{pmatrix} 1 & 0 & 0 \\ 0 & -2 & 0 \\ 0 & 0 & 1 \end{pmatrix}$	$\begin{pmatrix} 0 & 1 & 2 \\ 1 & 0 & -1 \\ 2 & -1 & 0 \end{pmatrix}$	$\begin{pmatrix} \sqrt{\frac{5}{2}} & 0 & 0 \\ 0 & 0 & 0 \\ 0 & \sqrt{\frac{5}{2}} & 0 \end{pmatrix}$	$\begin{pmatrix} 0 & -\sqrt{\frac{2}{5}} & -\sqrt{\frac{21}{10}} \\ -\frac{1}{\sqrt{10}} & \frac{1}{\sqrt{10}} & -2\sqrt{\frac{6}{35}} \\ -\sqrt{\frac{2}{5}} & 0 & -\sqrt{\frac{18}{14}} \end{pmatrix}$	$\begin{pmatrix} -\frac{3}{2} & 0 & 0 \\ 0 & -\frac{3}{2} & 0 \\ 0 & 0 & 1 \end{pmatrix}$	$\begin{pmatrix} 0 & -\frac{3}{5} & -\frac{3\sqrt{21}}{10} \\ -\frac{3}{5} & 0 & -\frac{3}{2}\sqrt{\frac{3}{7}} \\ -\frac{3\sqrt{21}}{10} & -\frac{3}{2}\sqrt{\frac{3}{7}} & -\frac{4}{7} \end{pmatrix}$
$\frac{5}{2}^+$	$-$	$-$	$-$	$-$	$\begin{pmatrix} 1 & 0 & 0 \\ 0 & -\frac{3}{2} & 0 \\ 0 & 0 & 1 \end{pmatrix}$	$\begin{pmatrix} 0 & \frac{3}{5}\sqrt{\frac{7}{2}} & \frac{2\sqrt{14}}{5} \\ \frac{3}{5}\sqrt{\frac{7}{2}} & -\frac{3}{7} & -\frac{3}{7} \\ \frac{2\sqrt{14}}{5} & -\frac{3}{7} & \frac{4}{7} \end{pmatrix}$
$\frac{7}{2}^-$	$-$	$-$	$-$	$-$	(1)	$(-\frac{2}{5})$

$$-C_4 \mathcal{A}_4 Y_{\Lambda, m_V}, \quad (22)$$

$$\mathcal{V}_{\bar{D}_1 B \rightarrow \bar{D}_2 B}^\pi = -\frac{C_2}{3\sqrt{3}} (\mathcal{A}_7 Z_{\Lambda, m_P} + \mathcal{A}_8 T_{\Lambda, m_P}), \quad (23)$$

$$\mathcal{V}_{\bar{D}_1 B \rightarrow \bar{D}_2 B}^\rho = -\frac{\sqrt{6} C_3}{18} (2\mathcal{A}_7 Z_{\Lambda, m_P} + \mathcal{A}_8 T_{\Lambda, m_P}). \quad (24)$$

Here, we have defined several coupling constants, operators, and useful functions, whose explicit forms are

$$C_1 = g_\sigma g_{\sigma BB}, \quad C_2 = \frac{g_{BBP} k}{f_\pi m_{\pi, \eta}}, \quad C_4 = g_{BBV} \beta'' g_V, \quad (25)$$

$$C_3 = \frac{5\lambda'' g_V}{9} \left(\frac{g_{BBV}}{2m_2} + \frac{g_{BBV}}{2m_4} + \frac{f_{BBV}}{m_B} \right), \quad (26)$$

$$\mathcal{A}_1 = \chi_4^\dagger \chi_3^\dagger \epsilon_3^\dagger \cdot \epsilon_1 \chi_2 \chi_1, \quad (27)$$

$$\mathcal{A}_2 = \chi_4^\dagger \chi_3^\dagger (i\epsilon_1 \times \epsilon_3^\dagger \cdot \boldsymbol{\sigma}) \chi_2 \chi_1, \quad (28)$$

$$\mathcal{A}_3 = \chi_4^\dagger \chi_3^\dagger S(i\epsilon_1 \times \epsilon_3^\dagger, \boldsymbol{\sigma}, \hat{r}) \chi_2 \chi_1, \quad (29)$$

$$\mathcal{A}_4 = \sum_{m, n, a, b} C_{1m, 1n}^{2, m+n} C_{1a, 1b}^{2, a+b} \chi_4^\dagger \chi_3^\dagger (\epsilon_1^a \cdot \epsilon_3^{m\dagger}) (\epsilon_1^b \cdot \epsilon_3^{n\dagger}) \chi_2 \chi_1, \quad (30)$$

$$\mathcal{A}_5 = \sum_{m, n, a, b} C_{1m, 1n}^{2, m+n} C_{1a, 1b}^{2, a+b} \chi_4^\dagger \chi_3^\dagger (\epsilon_1^a \cdot \epsilon_3^{m\dagger}) (i\epsilon_1^b \times \epsilon_3^{n\dagger}) \cdot \boldsymbol{\sigma} \chi_2 \chi_1, \quad (31)$$

$$\mathcal{A}_6 = \sum_{m, n, a, b} C_{1m, 1n}^{2, m+n} C_{1a, 1b}^{2, a+b} \chi_4^\dagger \chi_3^\dagger (\epsilon_1^a \cdot \epsilon_3^{m\dagger}) \times S(i\epsilon_1^b \times \epsilon_3^{n\dagger}, \boldsymbol{\sigma}, \hat{r}) \chi_2 \chi_1, \quad (32)$$

$$\mathcal{A}_7 = \sum_{m, n, a, b} C_{1m, 1n}^{2, m+n} \chi_4^\dagger \chi_3^\dagger (\epsilon_1 \cdot \epsilon_3^{m\dagger}) (\epsilon_3^{n\dagger} \cdot \boldsymbol{\sigma}) \chi_2 \chi_1, \quad (33)$$

$$\mathcal{A}_8 = \sum_{m, n, a, b} C_{1m, 1n}^{2, m+n} \chi_4^\dagger \chi_3^\dagger (\epsilon_1 \cdot \epsilon_3^{m\dagger}) S(\epsilon_3^{n\dagger}, \boldsymbol{\sigma}, \hat{r}) \chi_2 \chi_1, \quad (34)$$

$$Y_{\Lambda, m} = \frac{1}{4\pi r} (e^{-mr} - e^{-\Lambda r}) - \frac{\Lambda^2 - m^2}{8\pi\Lambda} e^{-\Lambda r}, \quad (35)$$

$$T_{\Lambda, m} = r \frac{\partial}{\partial r} \frac{1}{r} \frac{\partial}{\partial r} Y_{\Lambda, m}, \quad Z_{\Lambda, m} = \nabla^2 Y_{\Lambda, m}. \quad (36)$$

When performing the numerical calculations, the operators in Eq. (27)-(34) will be replaced by numerical matrices, which are summarized in Table IV.

III. NUMERICAL RESULTS

Following the derivation of the one-boson-exchange (OBE) effective potentials, we investigate the possible existence of anti-charm molecular pentaquarks with strangeness $|S| = 0, 1,$ and 2 . We numerically solve the coupled-channel Schrödinger equations to search for bound state solutions, and the identification criteria on the loosely bound molecules are a binding energy E on the order of several to several tens of MeV and a root-mean-square (RMS) radius r_{RMS} of approximately 1.00 fm or larger. In our analysis, the cutoff parameter Λ is varied within the range $\Lambda \leq 2.00$ GeV. Drawing upon the established phenomenology of nucleon-nucleon interactions [55, 56], we regard loosely bound states that emerge with a cutoff $\Lambda \sim 1.00$ GeV as the most promising candidates for anti-charm molecular pentaquarks.

A. The \bar{D}_1N and \bar{D}_2^*N systems

The bound state solutions for the \bar{D}_1N and \bar{D}_2^*N systems, incorporating S - D wave mixing and P -wave interactions, are summarized in Table V, where the analyzed quantum number configurations are $J^P = 1/2^\pm, 3/2^\pm,$ and $5/2^-$ for \bar{D}_1N , and $1/2^-, 3/2^\pm, 5/2^\pm,$ and $7/2^-$ for \bar{D}_2^*N .

For a cutoff $\Lambda \sim 1.00$ GeV, we can obtain bound state solutions for the \bar{D}_1N systems with $I(J^P) = 0(1/2^\pm, 3/2^+), 1(1/2^\pm, 3/2^+),$ and $0(3/2^-)$. The corresponding binding energies range from several to several tens of MeV, with RMS radii on the order of 1.00 fm or larger, consistent with the properties of loosely bound molecular states. A comparison of cutoff values reveals a systematic pattern: for identical spin-parity with the S -wave interactions, the required cutoff is smaller for isoscalar states than for isovector states, e.g., $\Lambda(0(1/2^+)) < \Lambda(1(1/2^+))$ and $\Lambda(0(3/2^+)) < \Lambda(1(3/2^+))$. This indicates that the OBE effective potentials are more attractive in the isoscalar channels. Furthermore, S -wave states generally exhibit deeper binding than P -wave states with the same isospin and total spin, as evidenced by relations such as $\Lambda(0(1/2^+)) < \Lambda(0(1/2^-))$. As for the \bar{D}_1N systems with $0(5/2^-)$ and $1(3/2^-, 5/2^-)$, no bound state solutions are found within $\Lambda \leq 2.00$ GeV, indicating insufficient attraction in these channels.

Next, we perform a coupled-channel analysis for the \bar{D}_1N/\bar{D}_2^*N systems. For the channels $I(J^P) = 0(1/2^\pm), 1(1/2^\pm), 0(3/2^+), 1(3/2^+),$ and $0(3/2^-)$, the binding energies increase slightly compared to the single-channel \bar{D}_1N results, while the qualitative features of the bound states remain unchanged. This confirms the molecular nature of these states and demonstrates that coupled-channel effects provide additional attractive contributions. For the systems with $1(5/2^-)$, bound states remain elusive even after considering the coupled channel effects.

However, the coupled-channel calculation yields bound solutions for the $1(3/2^-)$ and $0(5/2^-)$ configurations. These states are dominated by the \bar{D}_2^*N component and are characterized by RMS radii smaller than 1.00 fm. Their compact size is inconsistent with a loosely bound molecular configura-

tion. Therefore, they are not considered promising molecular candidates despite the presence of a sufficiently attractive potential.

Thus, we now focus on possible molecular states predominantly composed of \bar{D}_2^*N . As shown in the right panel of Table V, we find strong attractive interactions supporting loosely bound states for the \bar{D}_2^*N systems with $1(3/2^-)$ and $0(5/2^-)$, with binding energies from several to tens of MeV, RMS radii around or above 1.00 fm, and reasonable cutoff parameters, which all indicate that these two states qualify as promising molecular candidates.

In addition, we can identify six further \bar{D}_2^*N molecular candidates with quantum numbers $I(J^P) = 0(1/2^-, 3/2^\pm, 5/2^+)$ and $1(3/2^+, 5/2^+)$, all of which can yield loosely bound solutions within a reasonable cutoff range. Consistent with the \bar{D}_1N findings, the analysis of cutoff values suggests that S -wave isoscalar configurations are the most favorable for molecular formation. For the \bar{D}_2^*N systems with $0(7/2^-)$ and $1(1/2^-, 5/2^-, 7/2^-)$, no bound states can be found within $\Lambda \leq 2.00$ GeV, implying that the OBE potentials in these channels lack sufficient strength.

In summary, we propose the following systems as promising anti-charm molecular pentaquark candidates:

- \bar{D}_1N states with $I(J^P) = 0, 1(1/2^\pm, 3/2^+)$ and $0(3/2^-)$.
- \bar{D}_2^*N states with $I(J^P) = 0, 1(3/2^\pm, 5/2^+)$ and $0(1/2^-, 5/2^-)$.

B. The $\bar{D}_1\Lambda, \bar{D}_1\Sigma, \bar{D}_2^*\Lambda$ and $\bar{D}_2^*\Sigma$ systems

Compared to the $\bar{T}N$ systems, the $\bar{T}\Lambda$ interactions lack contributions from π and ρ meson exchange due to the isospin-forbidden $\Lambda\Lambda\pi(\rho)$ vertex. This absence of key short- and intermediate-range forces is expected to weaken the effective potential, making bound-state formation less likely in a single-channel analysis. For the $\bar{T}\Sigma$ systems, π and ρ exchange is permitted. However, the reduced number of light u/d quarks in the Σ hyperon relative to the nucleon may also lead to somewhat weaker OBE potentials compared to the $\bar{T}N$ case. Consequently, while single-channel $\bar{T}\Lambda$ molecules appear improbable, the introduction of coupled-channel effects with $\bar{T}\Sigma$ channels may yield viable $\bar{T}\Lambda/\bar{T}\Sigma$ molecular candidates dominated by the lower $\bar{T}\Lambda$ threshold, as well as single $\bar{T}\Sigma$ molecules.

To verify the above analysis, a single-channel analysis of the $\bar{D}_1\Lambda$ and $\bar{D}_2^*\Lambda$ systems across the cutoff range $0.80 \leq \Lambda \leq 2.00$ GeV is performed which yields no bound state solutions for any of the considered quantum numbers, confirming the insufficient attraction from $\sigma, \omega,$ and ϕ exchange alone.

However, bound states emerge when $\bar{T}\Sigma$ channels are coupled. As shown in Table VI, we find loosely bound solutions for the coupled $\bar{D}_1\Lambda/\bar{D}_2^*\Lambda/\bar{D}_1\Sigma/\bar{D}_2^*\Sigma$ systems with $I(J^P) = 1/2(1/2^\pm, 3/2^+)$ and the coupled $\bar{D}_2^*\Lambda/\bar{D}_1\Sigma/\bar{D}_2^*\Sigma$ systems with $1/2(3/2^+, 5/2^+)$. For these states, the dominant component is the lowest $\bar{T}\Lambda$ channel. With binding energies of several MeV and RMS radii on the order of 1.00 fm or larger, these systems satisfy the criteria for loosely bound molecules and

TABLE V: The bound state solutions for the $\bar{T}N$ systems. Here, the unites for the cutoff Λ , the binding energy E , and the root-mean-square radius r_{RMS} are GeV, MeV, and fm, respectively. Channels that are forbidden or dominant are marked with the symbols “-” and in bold manner, respectively. The masses thresholds for the involved channels are $m_{\bar{D}_1N} = 3360.27$ MeV, and $m_{\bar{D}_2^*N} = 3401.32$ MeV, respectively.

$I(J^P)$	Λ	E	r_{RMS}	$\bar{D}_1N(^2S/^4D)$	$I(J^P)$	Λ	E	r_{RMS}	$\bar{D}_2^*N(^4S/^4D/^6D)$
$0(\frac{1}{2}^+)$	0.78	-9.57	1.51	99.09 /0.91	$0(\frac{3}{2}^+)$	0.78	-6.77	1.76	98.32 /0.23/1.45
	0.79	-11.39	1.41	99.08 /0.92		0.79	-8.26	1.63	98.27 /0.25/1.48
$1(\frac{1}{2}^+)$	1.33	-0.51	4.72	97.80 /2.20	$1(\frac{3}{2}^+)$	1.33	-1.42	3.29	96.03 /0.77/3.20
	1.35	-8.13	1.40	94.75 /5.25		1.34	-3.95	2.04	94.36 /1.11/4.53
$I(J^P)$	Λ	E	r_{RMS}	$\bar{D}_1N(^4S/^2D/^4D)$	$I(J^P)$	Λ	E	r_{RMS}	$\bar{D}_2^*N(^6S/^4D/^6D)$
$0(\frac{3}{2}^+)$	1.05	-1.17	4.00	95.52 /0.65/3.83	$0(\frac{5}{2}^+)$	1.05	-1.52	3.63	94.30 /1.62/4.08
	1.10	-5.31	2.16	92.15 /1.11/6.74		1.10	-6.55	2.00	90.22 /2.75/7.03
$1(\frac{3}{2}^+)$	1.45	-1.06	3.93	95.64 /1.03/3.33	$1(\frac{5}{2}^+)$	1.50	-2.08	3.00	94.75 /2.21/3.04
	1.50	-4.03	2.26	92.00 /1.95/6.05		1.55	-5.57	1.99	91.88 /3.48/4.64
$I(J^P)$	Λ	E	r_{RMS}	$\bar{D}_1N(^2P/^4P)$	$I(J^P)$	Λ	E	r_{RMS}	$\bar{D}_2^*N(^4P/^6P)$
$0(\frac{1}{2}^-)$	1.66	-0.72	2.39	83.00 /17.00	$0(\frac{1}{2}^-)$	1.63	-1.75	1.98	100.00 /-
	1.70	-5.68	1.49	83.55 /16.45		1.66	-5.43	1.52	100.00 /-
$1(\frac{1}{2}^-)$	1.48	-1.35	2.14	17.57/ 82.43	$0(\frac{3}{2}^-)$	1.91	-0.67	2.33	69.68 /30.32
	1.65	-7.27	1.39	17.81/ 82.19		1.96	-7.37	1.33	70.40 /29.60
$0(\frac{3}{2}^-)$	1.28	-1.11	2.50	10.89/ 89.11	$1(\frac{3}{2}^-)$	1.53	-1.52	2.03	32.14 / 67.86
	1.3	-5.30	1.68	11.27 / 88.73		1.55	-6.90	1.39	32.97 / 67.03
$1(\frac{3}{2}^-)$	-	-	-	-/-	$0(\frac{5}{2}^-)$	1.21	-0.83	2.75	25.15 / 74.85
	-	-	-	-/-		1.24	-6.87	1.61	26.46 / 73.54
$0(\frac{5}{2}^-)$	-	-	-	-/-	$1(\frac{1}{2}^-)$	-	-	-	-/-
	-	-	-	-/-		$1(\frac{3}{2}^-)$	-	-	-
$1(\frac{5}{2}^-)$	-	-	-	-/-	$0(\frac{7}{2}^-)$		-	-	-
	-	-	-	-/-		$1(\frac{7}{2}^-)$	-	-	-

are identified as promising molecular candidates. Their existence underscores the crucial role of coupled-channel effects in providing the necessary attraction.

In contrast, for the P -wave coupled $\bar{D}_1\Lambda/\bar{D}_2^*\Lambda/\bar{D}_1\Sigma/\bar{D}_2^*\Sigma$ systems with $1/2(3/2^-, 5/2^-)$ and the $\bar{D}_2^*\Lambda/\bar{D}_1\Sigma/\bar{D}_2^*\Sigma$ systems with $1/2(1/2^-, 3/2^-, 5/2^-)$, bound solutions obtained near $\Lambda \sim 1.00$ GeV are dominated by the heavier $\bar{T}\Sigma$ components. This results in compact configurations with RMS radii significantly below 1.00 fm, which are incompatible with a molecular interpretation. Finally, no bound states are found for the $\bar{D}_2^*\Lambda/\bar{D}_1\Sigma/\bar{D}_2^*\Sigma$ system with $1/2(7/2^-)$ within the studied cutoff range.

We now investigate possible molecular states dominated by $\bar{T}\Sigma$ components. The bound state solutions for single-channel $\bar{D}_1\Sigma$ and $\bar{D}_2^*\Sigma$ systems are collected in Table VII for $0.80 \leq \Lambda \leq 2.00$ GeV, where Loosely bound states are found as

- $\bar{D}_1\Sigma$ states with $I(J^P) = 1/2, 3/2(1/2^\pm, 3/2^+)$ and $1/2(3/2^-)$.
- $\bar{D}_2^*\Sigma$ states with $I(J^P) = 1/2, 3/2(3/2^+, 5/2^+)$, $1/2(1/2^-, 5/2^-)$, and $1/2, 3/2(3/2^-)$.

These states, characterized by reasonable cutoff values, binding energies of several MeV, and RMS radii around 1.00 fm, qualify as good molecular candidates.

A subsequent coupled-channel analysis of the $\bar{D}_1\Sigma/\bar{D}_2^*\Sigma$ systems shows that the binding energies increase modestly, but the qualitative features of the states remain largely unchanged. This indicates that while coupled-channel effects provide a positive, attractive contribution, they are not essential for the formation of these particular $\bar{T}\Sigma$ molecules.

For P -wave $\bar{D}_1\Sigma$ with $1/2(5/2^-)$, $3/2(3/2^-, 5/2^-)$ or $\bar{D}_2^*\Sigma$ with $1/2(7/2^-)$, $3/2(1/2^-, 5/2^-, 7/2^-)$, no single-channel

TABLE VI: The bound state solutions for the $\bar{T}\Lambda$ systems. Here, the unites for the cutoff Λ , the binding energy E , and the root-mean-square radius r_{RMS} are GeV, MeV, and fm, respectively. Channels that are forbidden or dominant are marked with the symbols “-” and in bold manner, respectively. The masses thresholds for the involved channels are $m_{\bar{D}_1\Sigma} = 3537.68$ MeV, $m_{\bar{D}_2^*\Sigma} = 3578.73$ MeV, $m_{\bar{D}_1\Lambda} = 3615.15$ MeV and $m_{\bar{D}_2^*\Lambda} = 3656.20$ MeV respectively.

$I(J^P)$	Λ	E	r_{RMS}	$\bar{D}_1\Lambda(^2S/^4D)$	$\bar{D}_2^*\Lambda(^4D/^6D)$	$\bar{D}_1\Sigma(^2S/^4D)$	$\bar{D}_2^*\Sigma(^4D/^6D)$
$\frac{1}{2}(\frac{1}{2}^+)$	1.10	-0.90	3.67	84.19 /0.16	~ 0 /0.02	15.06/0.55	~ 0 /0.02
	1.15	-2.86	2.01	62.51 /0.50	~ 0 /0.05	35.88/1.03	~ 0 /0.03
$\frac{1}{2}(\frac{3}{2}^+)$	1.20	-0.37	5.13	96.66 / ~ 0 /0.09	0.13/ ~ 0 / ~ 0	1.28/1.77 /0.88	0.78/ ~ 0 /0.01
	1.24	-4.80	1.68	65.21 /0.14/0.98	1.04 /0.02 /0.15	16.53 /0.61 / 3.28	11.85 / 0.02 / 0.17
$\frac{1}{2}(\frac{1}{2}^-)$	1.73	-0.39	2.00	4.86/ 67.29	-/0.02	17.07 / 10.29	-/0.47
	1.75	-6.05	1.11	4.87/ 62.02	-/0.02	20.76 / 11.77	-/0.56
$\frac{1}{2}(\frac{3}{2}^-)$	1.46	-3.04	1.16	4.07/38.72	0.05/0.02	6.48/ 50.55	0.14/0.07
	1.47	-8.10	0.96	3.63/35.50	0.05/0.02	6.78/ 53.78	0.16/0.08
$\frac{1}{2}(\frac{5}{2}^-)$	1.47	-1.95	0.73	-/ ~ 0	6.86/25.70	-/0.01	17.25/ 50.18
	1.48	-9.25	0.71	-/ ~ 0	6.60/25.25	-/ ~ 0	17.23/ 50.92
$\frac{1}{2}(\frac{3}{2}^+)$	1.10	-2.69	2.22		74.28 /0.05 /0.40	0.19/ ~ 0 /0.01	23.62/0.20/1.25
	1.13	-5.29	1.55		59.05 /0.10/0.71	0.26 / ~ 0 /0.01	37.88 /0.27 / 1.72
$\frac{1}{2}(\frac{5}{2}^+)$	1.20	-0.47	4.89		97.44 /0.03 /0.11		1.14/0.41/0.87
	1.25	-7.02	1.53		73.08 /0.43/1.28		19.20 /1.81 / 4.20
$\frac{1}{2}(\frac{1}{2}^-)$	1.84	-1.36	1.25		33.98/-	4.39/0.88	60.75 /-
	1.86	-5.87	0.96		29.79/-	4.65/0.95	64.61 /-
$\frac{1}{2}(\frac{3}{2}^-)$	1.61	-2.36	0.87		1.88 /5.90	10.33/ 76.77	3.23/ 1.89
	1.62	-7.06	0.82		2.09/5.98	10.15/ 76.14	3.60/2.04
$\frac{1}{2}(\frac{5}{2}^-)$	1.40	-1.84	1.33		10.76/ 35.17	0.02	14.87 / 39.18
	1.41	-6.53	1.03		9.61/ 31.95	0.01	15.93 / 42.50
$\frac{1}{2}(\frac{7}{2}^-)$	-	-	-		-/-		-/-

bound states can be found. However, when the coupled channel effects are further introduced, bound solutions appear for the $\bar{D}_1\Sigma/\bar{D}_2^*\Sigma$ systems with $1/2(5/2^-)$ and $3/2(3/2^-)$. Unfortunately, in these cases, the $\bar{D}_1\Sigma$ component is not dominant, and the resulting RMS radii deviate significantly from 1.00 fm. Therefore, these coupled states are not considered suitable molecular candidates.

C. The $\bar{D}_1\Xi$ and $\bar{D}_2^*\Xi$ systems

For the $\bar{T}\Xi$ systems, the reduced mass is somewhat larger than for $\bar{T}N$, which makes it a factor generally favors binding. However, the OBE effective potentials are expected to be weaker due to the reduced number of light u/d quarks in the Ξ hyperon, diminishing the effects from light meson exchange.

The bound state solutions for the $\bar{T}\Xi$ systems, incorporat-

TABLE VII: The bound state solutions for the $\bar{T}\Sigma$ systems. Here, the unites for the cutoff Λ , the binding energy E , and the root-mean-square radius r_{RMS} are GeV, MeV, and fm, respectively. Channels that are forbidden or dominant are marked with the symbols “-” and in bold manner, respectively. The masses thresholds for the involved channels are $m_{\bar{D}_1\Sigma} = 3615.15$ MeV and $m_{\bar{D}_2^*\Sigma} = 3656.20$ MeV respectively.

$I(J^P)$	Λ	E	r_{RMS}	$\bar{D}_1\Sigma(^2S/^4D)$	$I(J^P)$	Λ	E	r_{RMS}	$\bar{D}_2^*\Sigma(^4S/^4D/^6D)$
$\frac{1}{2}(\frac{1}{2}^+)$	0.83	-0.91	3.82	99.60 /0.40	$\frac{1}{2}(\frac{3}{2}^+)$	0.85	-1.43	3.18	99.20 /0.11/0.68
	0.89	-6.05	1.72	99.40 /0.60		0.90	-5.91	1.75	98.91 /0.16/0.93
$\frac{3}{2}(\frac{1}{2}^+)$	1.38	-0.46	4.70	97.68 /2.32	$\frac{3}{2}(\frac{3}{2}^+)$	1.35	-0.13	5.91	98.16 /0.35/1.49
	1.41	-7.02	1.45	93.92 /6.08		1.39	-5.34	1.71	93.25 /1.34/5.41
$I(J^P)$	Λ	E	r_{RMS}	$\bar{D}_1\Sigma(^4S/^2D/^4D)$	$I(J^P)$	Λ	E	r_{RMS}	$\bar{D}_2^*\Sigma(^6S/^4D/^6D)$
$\frac{1}{2}(\frac{3}{2}^+)$	1.05	-0.49	4.91	98.50 /0.25/1.25	$\frac{1}{2}(\frac{5}{2}^+)$	1.10	-2.56	2.65	96.88 /0.99/2.13
	1.15	-8.29	1.63	96.10 /0.66/3.24		1.13	-5.15	1.98	96.06 /1.24/2.70
$\frac{3}{2}(\frac{3}{2}^+)$	1.40	-0.96	3.83	96.24 /0.89/2.87	$\frac{3}{2}(\frac{5}{2}^+)$	1.40	-0.49	4.78	97.47 /1.05/1.48
	1.50	-6.36	1.76	90.91 /2.22/6.87		1.50	-4.22	2.08	93.22 /2.89/3.89
$I(J^P)$	Λ	E	r_{RMS}	$\bar{D}_1\Sigma(^2P/^4P)$	$I(J^P)$	Λ	E	r_{RMS}	$\bar{D}_2^*\Sigma(^4P/^6P)$
$\frac{1}{2}(\frac{1}{2}^-)$	1.75	-0.19	2.65	82.55 /17.45	$\frac{1}{2}(\frac{1}{2}^-)$	1.72	-1.02	1.99	100.00 /-
	1.80	-5.08	1.36	82.30 /17.00		1.77	-6.06	1.30	100.00 /-
$\frac{3}{2}(\frac{1}{2}^-)$	1.48	-0.45	2.60	17.76/ 82.24	$\frac{1}{2}(\frac{3}{2}^-)$	1.94	-1.41	1.80	68.64 /31.36
	1.52	-8.20	1.31	18.16/ 81.84		1.98	-5.26	1.31	68.90 /31.10
$\frac{1}{2}(\frac{3}{2}^-)$	1.48	-0.02	3.31	11.75/ 88.25	$\frac{3}{2}(\frac{3}{2}^-)$	1.54	-1.35	2.00	32.37/ 67.63
	1.53	-7.63	1.33	12.31/ 87.69		1.57	-7.67	1.30	33.08/ 66.92
$\frac{3}{2}(\frac{3}{2}^-)$	-	-	-	-/-	$\frac{1}{2}(\frac{5}{2}^-)$	1.41	-0.05	3.31	26.69/ 73.31
$\frac{1}{2}(\frac{5}{2}^-)$	-	-	-	-/-	1.45	-5.81	1.46	28.02/ 71.98	
$\frac{3}{2}(\frac{5}{2}^-)$	-	-	-	-/-	$\frac{3}{2}(\frac{1}{2}^-)$	-	-	-	-/-
					$\frac{3}{2}(\frac{5}{2}^-)$	-	-	-	-/-
					$\frac{1}{2}(\frac{7}{2}^-)$	-	-	-	-/-
					$\frac{3}{2}(\frac{7}{2}^-)$	-	-	-	-/-

ing S - D wave mixing and P -wave interactions, are presented in Table VIII. For a cutoff $\Lambda \sim 1.00$ GeV, we obtain loosely bound solutions for the $\bar{D}_1\Xi$ states with $I(J^P) = 0(1/2^\pm, 3/2^+)$ and $1(3/2^+)$ and the $\bar{D}_2^*\Xi$ states with $0(3/2^\pm, 5/2^+)$ and $1(5/2^+)$. A comparison with the $\bar{T}N$ systems reveals that, for identical binding energies, the required cutoff values are slightly larger for the corresponding $\bar{T}\Xi$ states. This cutoff hierarchy confirms that the OBE potentials are indeed somewhat less attractive in the $\bar{T}\Xi$ sector. The RMS radii of the states listed above are consistent with the typical size of a loosely bound molecule. Therefore, we identify them as promising molecular candidates.

Furthermore, we observe that for the positive-parity bound states, the S -wave channel provides the dominant compo-

nent. In contrast, for the negative-parity states, the higher-spin channels exhibit the largest probabilities.

While for the $\bar{D}_1\Xi$ systems with $0(3/2^-, 5/2^-)$ and $1(1/2^+, 1/2^-, 3/2^-, 5/2^-)$, and the $\bar{D}_2^*\Xi$ systems with $0(1/2^-, 5/2^-, 7/2^-)$ and $1(1/2^-, 3/2^+, 3/2^-, 5/2^-, 7/2^-)$, no bound state solutions are found within a reasonable cutoff range. This indicates that the OBE effective potentials for these channels lack sufficient strength to form molecular states. This conclusion remains unchanged even after including coupled-channel effects for the $\bar{D}_1\Xi/\bar{D}_2^*\Xi$ systems with $0(3/2^-, 5/2^-)$ and $1(1/2^+, 1/2^-, 3/2^-, 5/2^-)$.

TABLE VIII: The bound state solutions for the $\bar{T}\Xi$ systems after considering the $S - D$ wave mixing effects and the P -wave interactions. Here, the unites for the cutoff Λ , the binding energy E , and the root-mean-square radius r_{RMS} are GeV, MeV, and fm, respectively. Channels that are forbidden or dominant are marked with the symbols “-” and in bold manner, respectively. The masses thresholds for the involved channels are $m_{\bar{D}_1\Xi} = 3740.29$ MeV, and $m_{\bar{D}_2^*\Xi} = 3781.34$ MeV, respectively.

$I(J^P)$	Λ	E	r_{RMS}	$\bar{D}_1\Xi(^2S/{}^4D)$	$I(J^P)$	Λ	E	r_{RMS}	$\bar{D}_2^*\Xi(^4S/{}^4D/{}^6D)$
$0(\frac{1}{2}^+)$	1.10	-2.96	2.33	99.80 /0.20	$0(\frac{3}{2}^+)$	1.06	-0.76	4.13	99.81 /0.03/0.16
	1.11	-3.96	2.06	99.78 /0.22		1.12	-5.91	1.74	99.63 /0.06/0.31
$1(\frac{1}{2}^+)$	-	-	-	-/-	$1(\frac{3}{2}^+)$	-	-	-/-	-/-
$I(J^P)$	Λ	E	r_{RMS}	$\bar{D}_1\Xi(^4S/{}^2D/{}^4D)$	$I(J^P)$	Λ	E	r_{RMS}	$\bar{D}_2^*\Xi(^6S/{}^4D/{}^6D)$
$0(\frac{3}{2}^+)$	1.00	-1.02	3.66	99.74 /0.05/0.21	$0(\frac{5}{2}^+)$	1.01	-1.87	2.83	99.69 /0.11/0.20
	1.05	-4.16	2.03	99.60 /0.08/0.32		1.09	-8.64	1.51	99.52 /0.18/0.30
$1(\frac{3}{2}^+)$	1.70	-0.81	3.95	98.88 /0.18/0.94	$1(\frac{5}{2}^+)$	1.70	-1.58	2.98	98.32 /0.51/1.17
	1.90	-8.47	1.44	96.28 /0.55/3.17		1.80	-5.50	1.72	96.78 /0.95/2.27
$I(J^P)$	Λ	E	r_{RMS}	$\bar{D}_1\Xi(^2P/{}^4P)$	$I(J^P)$	Λ	E	r_{RMS}	$\bar{D}_2^*\Xi(^4P/{}^6P)$
$0(\frac{1}{2}^-)$	1.67	-0.65	2.25	18.23/ 81.77	$0(\frac{3}{2}^-)$	1.70	-0.92	2.05	33.39/ 66.61
	1.72	-7.17	1.25	19.29/ 80.71		1.75	-7.82	1.21	35.19/ 64.81
$1(\frac{1}{2}^-)$	-	-	-	-/-	$0(\frac{1}{2}^-)$	-	-	-	-/-
$0(\frac{3}{2}^-)$	-	-	-	-/-	$1(\frac{1}{2}^-)$	-	-	-	-/-
$1(\frac{3}{2}^-)$	-	-	-	-/-	$1(\frac{3}{2}^-)$	-	-	-	-/-
$0(\frac{5}{2}^-)$	-	-	-	-/-	$0(\frac{5}{2}^-)$	-	-	-	-/-
$1(\frac{5}{2}^-)$	-	-	-	-/-	$1(\frac{5}{2}^-)$	-	-	-	-/-
					$0(\frac{7}{2}^-)$	-	-	-	-/-
					$1(\frac{7}{2}^-)$	-	-	-	-/-

IV. SUMMARY

The study of pentaquarks is a rapidly evolving field that has seen significant progress in recent years, particularly in the identification of new exotic hadrons at high-energy colliders. While many pentaquark states have been observed experimentally, their detailed structure and theoretical models are still being developed. This area of research continues to be one of the most exciting frontiers in hadron physics.

In this work, we have systematically investigated the interactions between the P -wave anti-charmed mesons (\bar{D}_1, \bar{D}_2^*) and the light octet baryons (N, Λ, Σ, Ξ) within the framework of the OBE model. Our analysis incorporates the coupled-channel effects, the S - D wave mixing, and P -wave interactions. The relevant coupling constants are determined by extending the well-established nucleon-nucleon interaction parameters via the quark model and $SU(3)$ symmetry.

By numerically solving the coupled-channel Schrödinger equations, we can predict a series of promising anti-charmed

molecular pentaquark candidates with strangeness $|S| = 0, 1, 2$. As summarized in Figure 1, these candidates include

- $\bar{T}N$ molecules: \bar{D}_1N states with $I(J^P) = 0(1/2^\pm, 3/2^\pm), 1(1/2^\pm, 3/2^\pm)$; \bar{D}_2^*N states with $0(1/2^-, 3/2^\pm, 5/2^\pm), 1(3/2^\pm, 5/2^\pm)$.
- $\bar{T}\Sigma$ molecules: $\bar{D}_1\Sigma$ states with $1/2(1/2^\pm, 3/2^\pm), 3/2(1/2^\pm, 3/2^\pm)$; $\bar{D}_2^*\Sigma$ states with $1/2(1/2^-, 3/2^\pm, 5/2^\pm), 3/2(3/2^\pm, 5/2^\pm)$; $\bar{D}_1\Lambda/\bar{D}_2^*\Lambda/\bar{D}_1\Sigma/\bar{D}_2^*\Sigma$ coupled states with $1/2(1/2^\pm, 3/2^\pm)$ and $\bar{D}_2^*\Lambda/\bar{D}_1\Sigma/\bar{D}_2^*\Sigma$ coupled states with $1/2(3/2^\pm, 5/2^\pm)$.
- $\bar{T}\Xi$ molecules: $\bar{D}_1\Xi$ states with $0(1/2^\pm, 3/2^\pm), (3/2^\pm)$; $\bar{D}_2^*\Xi$ states with $0(3/2^\pm, 5/2^\pm), 1(5/2^\pm)$.

In addition, our analysis demonstrates that the coupled channel effects contribute actively to the formation of single channel molecular states and play an important role in the formation of coupled channel molecular states. Thus, experimental

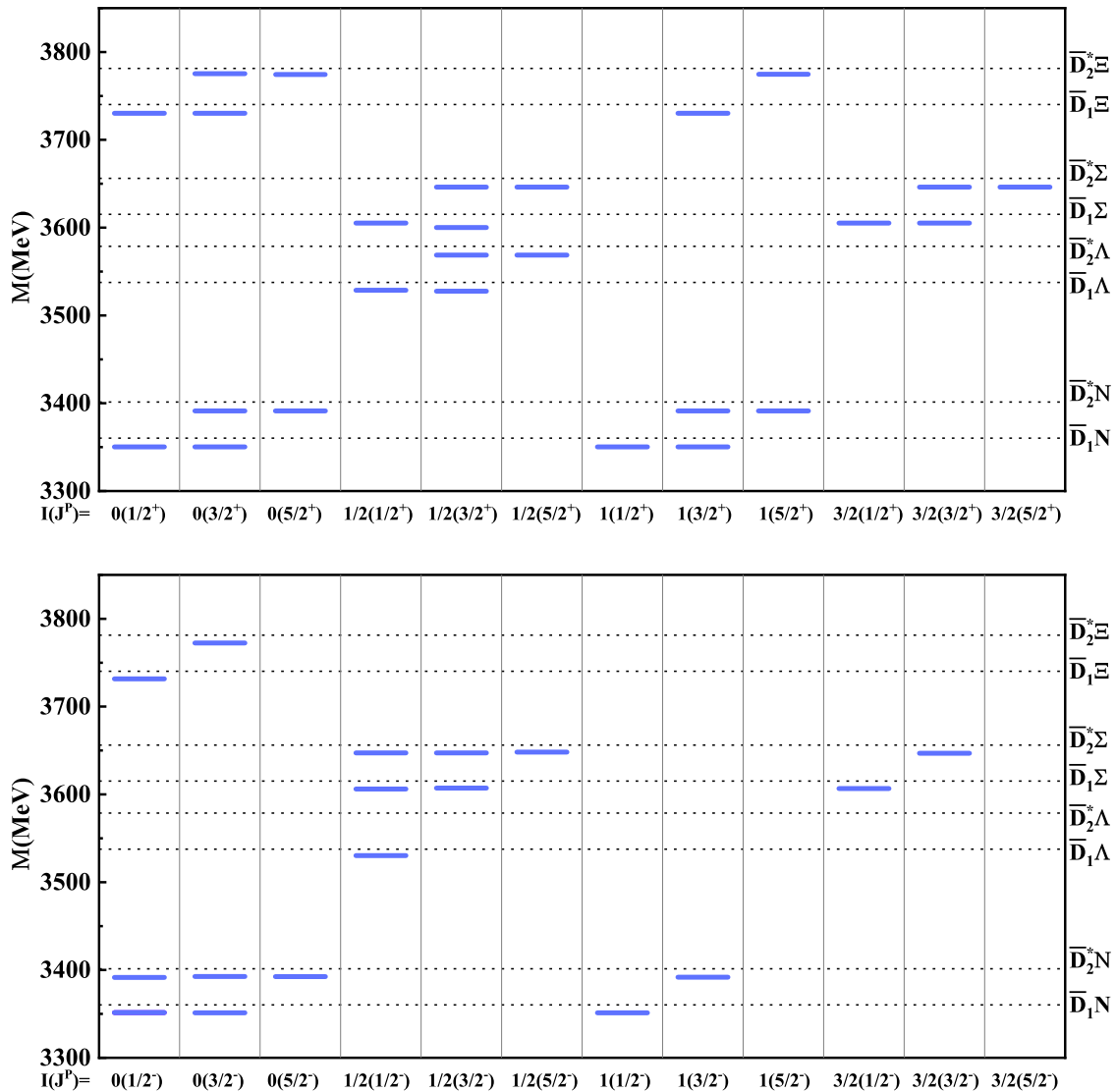


FIG. 1: Predictions of anti-charm pentaquarks.

search for the molecular pentaquarks predicted in this work will not only can test the molecular paradigm, but also can deepen our understanding on the non-perturbative interaction and coupled channel effects in multi-quark systems.

ACKNOWLEDGMENTS

This project is supported by the National Natural Science Foundation of China under Grants Nos. 12305139 and

12305087, and the Xiaoxiang Scholars Programme of Hunan Normal University.

[1] M. Gell-Mann, A Schematic Model of Baryons and Mesons, *Phys. Lett.* **8**, 214-215 (1964).

[2] G. Zweig, An SU(3) model for strong interaction symmetry and

its breaking. Version 1 [10.17181/CERN-TH-401](https://arxiv.org/abs/10.17181/CERN-TH-401) (1964).

[3] G. Zweig, An SU(3) model for strong interaction symmetry and its breaking. Version 2 [10.17181/CERN-TH-412](https://arxiv.org/abs/10.17181/CERN-TH-412) (1964).

- [4] D. Strottman, Multi - Quark Baryons and the MIT Bag Model, *Phys. Rev. D* **20**, 748-767 (1979).
- [5] H. J. Lipkin, New Possibilities for Exotic Hadrons: Anticharmed Strange Baryons, *Phys. Lett. B* **195**, 484-488 (1987).
- [6] C. Gignoux, B. Silvestre-Brac and J. M. Richard, Possibility of Stable Multi - Quark Baryons, *Phys. Lett. B* **193**, 323 (1987).
- [7] T. Nakano *et al.* [LEPS], Evidence for a narrow $S = +1$ baryon resonance in photoproduction from the neutron, *Phys. Rev. Lett.* **91**, 012002 (2003).
- [8] K. H. Hicks, On the conundrum of the pentaquark, *Eur. Phys. J. H* **37**, 1-31 (2012).
- [9] C. Alt *et al.* [NA49], Observation of an exotic $S = -2$, $Q = -2$ baryon resonance in proton proton collisions at the CERN SPS, *Phys. Rev. Lett.* **92**, 042003 (2004).
- [10] A. Aktas *et al.* [H1], Evidence for a narrow anti-charmed baryon state, *Phys. Lett. B* **588**, 17 (2004).
- [11] H. G. Fischer and S. Wenig, Are there $S = -2$ pentaquarks?, *Eur. Phys. J. C* **37**, 133-140 (2004).
- [12] M. I. Adamovich *et al.* [WA89], Search for the exotic Ξ -(1860) resonance in 340-GeV/c Sigma- nucleus interactions, *Phys. Rev. C* **70**, 022201 (2004).
- [13] S. Chekanov *et al.* [ZEUS], Search for a narrow charmed baryonic state decaying to $D^{*+}p^{-}$ in ep collisions at HERA, *Eur. Phys. J. C* **38**, 29-41 (2004).
- [14] R. Aaij *et al.* [LHCb], Observation of $J/\psi p$ Resonances Consistent with Pentaquark States in $\Lambda_b^0 \rightarrow J/\psi K^{-} p$ Decays, *Phys. Rev. Lett.* **115**, 072001 (2015).
- [15] R. Aaij *et al.* [LHCb], Observation of a narrow pentaquark state, $P_c(4312)^+$, and of two-peak structure of the $P_c(4450)^+$, *Phys. Rev. Lett.* **122** (2019) no.22, 222001 (2019).
- [16] R. Chen, X. Liu and S. L. Zhu, Hidden-charm molecular pentaquarks and their charm-strange partners, *Nucl. Phys. A* **954**, 406-421 (2016).
- [17] C. J. Xiao, Y. Huang, Y. B. Dong, L. S. Geng and D. Y. Chen, Exploring the molecular scenario of $P_c(4312)$, $P_c(4440)$, and $P_c(4457)$, *Phys. Rev. D* **100** no.1, 014022 (2019).
- [18] K. Chen, R. Chen, L. Meng, B. Wang and S. L. Zhu, Systematics of the heavy flavor hadronic molecules, *Eur. Phys. J. C* **82** no.7, 581 (2022).
- [19] H. W. Ke, F. Lu, H. Pang, X. H. Liu and X. Q. Li, Study on the possible molecular states composed of $\Lambda_c \bar{D}^*$, $\Sigma_c \bar{D}^*$, $\Xi_c \bar{D}^*$ and $\Xi_c' \bar{D}^*$ in the Bethe-Salpeter frame based on the pentaquark states $P_c(4440)$, $P_c(4457)$ and $P_{cs}(4459)$, *Eur. Phys. J. C* **83** no.11, 1074 (2023).
- [20] H. Xu, Q. Li, C. H. Chang and G. L. Wang, Recently observed P_c as molecular states and possible mixture of $P_c(4457)$, *Phys. Rev. D* **101** no.5, 054037 (2020).
- [21] R. Chen, Z. F. Sun, X. Liu and S. L. Zhu, Strong LHCb evidence supporting the existence of the hidden-charm molecular pentaquarks, *Phys. Rev. D* **100** no.1, 011502 (2019).
- [22] M. Z. Liu, Y. W. Pan, F. Z. Peng, M. Sánchez Sánchez, L. S. Geng, A. Hosaka and M. Pavon Valderrama, Emergence of a complete heavy-quark spin symmetry multiplet: seven molecular pentaquarks in light of the latest LHCb analysis, *Phys. Rev. Lett.* **122** no.24, 242001 (2019).
- [23] J. He, Study of $P_c(4457)$, $P_c(4440)$, and $P_c(4312)$ in a quasipotential Bethe-Salpeter equation approach, *Eur. Phys. J. C* **79** no.5, 393 (2019).
- [24] Y. Yamaguchi, H. García-Tecocoatzi, A. Giachino, A. Hosaka, E. Santopinto, S. Takeuchi and M. Takizawa, P_c pentaquarks with chiral tensor and quark dynamics, *Phys. Rev. D* **101** no.9, 091502 (2020).
- [25] T. J. Burns and E. S. Swanson, Molecular interpretation of the $P_c(4440)$ and $P_c(4457)$ states, *Phys. Rev. D* **100** no.11, 114033 (2019).
- [26] Y. H. Lin and B. S. Zou, Strong decays of the latest LHCb pentaquark candidates in hadronic molecule pictures, *Phys. Rev. D* **100** no.5, 056005 (2019).
- [27] C. W. Xiao, J. Nieves and E. Oset, Heavy quark spin symmetric molecular states from $\bar{D}^{(*)}\Sigma_c^{(*)}$ and other coupled channels in the light of the recent LHCb pentaquarks, *Phys. Rev. D* **100** no.1, 014021 (2019).
- [28] M. Karliner and J. L. Rosner, New strange pentaquarks, *Phys. Rev. D* **106** no.3, 036024 (2022).
- [29] X. K. Dong, F. K. Guo and B. S. Zou, A survey of heavy-antiheavy hadronic molecules, *Progr. Phys.* **41**, 65-93 (2021).
- [30] F. L. Wang and X. Liu, Emergence of molecular-type characteristic spectrum of hidden-charm pentaquark with strangeness embodied in the $P\psi s\Lambda(4338)$ and $Pcs(4459)$, *Phys. Lett. B* **835**, 137583 (2022).
- [31] M. J. Yan, F. Z. Peng, M. Sánchez Sánchez and M. Pavon Valderrama, $P\psi s\Lambda(4338)$ pentaquark and its partners in the molecular picture, *Phys. Rev. D* **107** no.7, 7 (2023).
- [32] C. Fernández-Ramírez *et al.* [JPAC], Interpretation of the LHCb $P_c(4312)^+$ Signal, *Phys. Rev. Lett.* **123** no.9, 092001 (2019).
- [33] M. L. Du, V. Baru, F. K. Guo, C. Hanhart, U. G. Meißner, J. A. Oller and Q. Wang, Interpretation of the LHCb P_c States as Hadronic Molecules and Hints of a Narrow $P_c(4380)$, *Phys. Rev. Lett.* **124** no.7, 072001 (2020).
- [34] H. X. Chen, W. Chen and S. L. Zhu, Possible interpretations of the $P_c(4312)$, $P_c(4440)$, and $P_c(4457)$, *Phys. Rev. D* **100** no.5, 051501 (2019).
- [35] Z. H. Guo and J. A. Oller, Anatomy of the newly observed hidden-charm pentaquark states: $P_c(4312)$, $P_c(4440)$ and $P_c(4457)$, *Phys. Lett. B* **793**, 144-149 (2019).
- [36] B. Wang, L. Meng and S. L. Zhu, Hidden-charm and hidden-bottom molecular pentaquarks in chiral effective field theory, *JHEP* **11**, 108 (2019).
- [37] L. Meng, B. Wang, G. J. Wang and S. L. Zhu, The hidden charm pentaquark states and $\Sigma_c \bar{D}^{(*)}$ interaction in chiral perturbation theory, *Phys. Rev. D* **100** no.1, 014031 (2019).
- [38] M. B. Voloshin, Some decay properties of hidden-charm pentaquarks as baryon-meson molecules, *Phys. Rev. D* **100** no.3, 034020 (2019).
- [39] Z. G. Wang and X. Wang, Analysis of the strong decays of the $P_c(4312)$ as a pentaquark molecular state with QCD sum rules, *Chin. Phys. C* **44**, 103102 (2020).
- [40] T. Gutsche and V. E. Lyubovitskij, Structure and decays of hidden heavy pentaquarks, *Phys. Rev. D* **100** no.9, 094031 (2019).
- [41] R. Zhu, X. Liu, H. Huang and C. F. Qiao, Analyzing doubly heavy tetra- and penta-quark states by variational method, *Phys. Lett. B* **797**, 134869 (2019).
- [42] G. J. Wang, L. Y. Xiao, R. Chen, X. H. Liu, X. Liu and S. L. Zhu, Probing hidden-charm decay properties of P_c states in a molecular scenario, *Phys. Rev. D* **102** no.3, 036012 (2020).
- [43] M. L. Du, V. Baru, F. K. Guo, C. Hanhart, U. G. Meißner, J. A. Oller and Q. Wang, Revisiting the nature of the P_c pentaquarks, *JHEP* **08**, 157 (2021).
- [44] C. W. Shen, D. Rönchen, U. G. Meißner, B. S. Zou and Y. F. Wang, Exploration of the LHCb P_c states and possible resonances in a unitary coupled-channel model, *Eur. Phys. J. C* **84** no.7, 764 (2024).
- [45] R. Molina, C. W. Xiao and E. Oset, J/ψ reaction mechanisms and suppression in the nuclear medium, *Phys. Rev. C* **86**, 014604 (2012).
- [46] Z. C. Yang, Z. F. Sun, J. He, X. Liu and S. L. Zhu, The possible hidden-charm molecular baryons composed of anti-charmed meson and charmed baryon, *Chin. Phys. C* **36**, 6-13 (2012).

- [47] J. J. Wu, R. Molina, E. Oset and B. S. Zou, Prediction of narrow N^* and Λ^* resonances with hidden charm above 4 GeV, *Phys. Rev. Lett.* **105**, 232001 (2010).
- [48] W. L. Wang, F. Huang, Z. Y. Zhang and B. S. Zou, $\Sigma_c \bar{D}$ and $\Lambda_c \bar{D}$ states in a chiral quark model, *Phys. Rev. C* **84**, 015203 (2011).
- [49] M. Karlner and J. L. Rosner, New Exotic Meson and Baryon Resonances from Doubly-Heavy Hadronic Molecules, *Phys. Rev. Lett.* **115** no.12, 122001 (2015).
- [50] X. Q. Li and X. Liu, A possible global group structure for exotic states, *Eur. Phys. J. C* **74** no.12, 3198 (2014).
- [51] R. Chen, Z. F. Sun, X. Liu and S. M. Gerasyuta, Predicting exotic molecular states composed of nucleon and P-wave charmed meson, *Phys. Rev. D* **90** no.3, 034011 (2014).
- [52] H. Y. Cheng and K. C. Yang, Charmless Hadronic B Decays into a Tensor Meson, *Phys. Rev. D* **83**, 034001 (2011).
- [53] Y. Y. Cui, X. M. Tang, Q. Huang and R. Chen, Emergence of charm-strange dibaryons with negative parity via baryon-baryon interactions, *Eur. Phys. J. C* **85** (2025) no.12, 1460
- [54] X. M. Tang, L. c. Sheng, Q. Huang and R. Chen, The recoil corrections, correlation functions and possible double-strange hadronic molecules,” *Phys. Lett. B* **870** (2025), 139896
- [55] N. A. Tornqvist, From the Deuteron to Deusons, an Analysis of Deuteron-like Meson Meson Bound States, *Z. Phys. C* **61**, 525 (1994).
- [56] N. A. Tornqvist, On Deusons or Deuteron-like Meson Meson Bound States, *Nuovo Cim. A* **107**, 2471 (1994).
- [57] J. Y. Huo, L. C. Sheng, R. Chen and X. Liu, Predicting possible molecular states of nucleons with Ξ_c , Ξ_c^* , and Ξ_c' , *Phys. Rev. D* **110** no.5, 054040 (2024).
- [58] Y. R. Liu and M. Oka, $\Lambda_c N$ bound states revisited, *Phys. Rev. D* **85**, 014015 (2012).
- [59] Y. R. Liu, X. Liu, W. Z. Deng, and S. L. Zhu, Is $X(3872)$ really a molecular state?, *Eur. Phys. J. C* **56**, 63 (2008).
- [60] C. E. Thomas and F. E. Close, Is $X(3872)$ a molecule?, *Phys. Rev. D* **78**, 034007 (2008).
- [61] X. Liu, Z. G. Luo, Y. R. Liu, and S. L. Zhu, $X(3872)$ and other possible heavy molecular states, *Eur. Phys. J. C* **61**, 411 (2009).
- [62] I. W. Lee, A. Faessler, T. Gutsche, and V. E. Lyubovitskij, $X(3872)$ as a molecular DD^* state in a potential model, *Phys. Rev. D* **80**, 094005 (2009).
- [63] R. Chen, X. Liu, X. Q. Li and S. L. Zhu, Identifying exotic hidden-charm pentaquarks, *Phys. Rev. Lett.* **115**, 132002 (2015).
- [64] R. Chen and X. Liu, Is the newly reported $X(5568)$ a $B\bar{K}$ molecular state?, *Phys. Rev. D* **94**, 034006 (2016).
- [65] K. Chen, R. Chen, Z. F. Sun and X. Liu, $\bar{K}\Lambda$ molecular explanation to the newly observed $\Xi(1620)^0$, *Phys. Rev. D* **100**, 074006 (2019).
- [66] R. Chen, Q. Huang, X. Liu and S. L. Zhu, Predicting another doubly charmed molecular resonance $T'_{cc}(3876)$, *Phys. Rev. D* **104**, 114042 (2021).
- [67] R. Chen, Can the newly reported $P_{cs}(4459)$ be a strange hidden-charm $\Xi_c \bar{D}^*$ molecular pentaquark?, *Phys. Rev. D* **103**, 054007 (2021).
- [68] R. Chen and Q. Huang, $Z_{cs}(3985)^-$: A strange hidden-charm tetraquark resonance or not?, *Phys. Rev. D* **103**, 034008 (2021).
- [69] R. Chen and Q. Huang, Charmoniumlike resonant explanation on the newly observed $X(3960)$, *Phys. Lett. B* **846**, 138254 (2023).
- [70] R. Chen and X. Liu, Mass behavior of hidden-charm open-strange pentaquarks inspired by the established P_c molecular states, *Phys. Rev. D* **105**, 014029 (2022).
- [71] F. L. Wang, R. Chen and X. Liu, Prediction of hidden-charm pentaquarks with double strangeness, *Phys. Rev. D* **103**, 034014 (2021).
- [72] F. L. Wang, R. Chen, Z. W. Liu and X. Liu, Probing new types of P_c states inspired by the interaction between S -wave charmed baryon and anti-charmed meson in a \bar{T} doublet, *Phys. Rev. C* **101**, 025201 (2020).
- [73] J. He, X. Liu, Z. F. Sun and S. L. Zhu, $Z_c(4025)$ as the hadronic molecule with hidden charm, *Eur. Phys. J. C* **73**, 2635 (2013).
- [74] N. Li, Z. F. Sun, X. Liu and S. L. Zhu, Coupled-channel analysis of the possible $D^{(*)}D^{(*)}$, $\bar{B}^{(*)}\bar{B}^{(*)}$ and $D^{(*)}\bar{B}^{(*)}$ molecular states, *Phys. Rev. D* **88**, 114008 (2013).
- [75] N. Li and S. L. Zhu, Hadronic molecular states composed of heavy flavor baryons, *Phys. Rev. D* **86**, 014020 (2012).
- [76] Z. F. Sun, X. Liu, M. Nielsen and S. L. Zhu, Hadronic molecules with both open charm and bottom, *Phys. Rev. D* **85**, 094008 (2012).
- [77] Z. F. Sun, J. He, X. Liu, Z. G. Luo and S. L. Zhu, $Z_b(10610)^{\pm}$ and $Z_b(10650)^{\pm}$ as the $B^* \bar{B}$ and $B^* \bar{B}^*$ molecular states, *Phys. Rev. D* **84**, 054002 (2011).
- [78] N. Lee, Z. G. Luo, X. L. Chen and S. L. Zhu, Possible deuteronlike molecular states composed of heavy baryons, *Phys. Rev. D* **84**, 014031 (2011).
- [79] X. Liu and S. L. Zhu, $Y(4143)$ is probably a molecular partner of $Y(3930)$, *Phys. Rev. D* **80**, 017502 (2009).
- [80] X. Liu, Y. R. Liu, W. Z. Deng and S. L. Zhu, $Z^+(4430)$ as a $D_1^* D^*(D_1 D^*)$ molecular state, *Phys. Rev. D* **77**, 094015 (2008).
- [81] P. Chen, Z. W. Liu, Z. L. Zhang, S. Q. Luo, F. L. Wang, J. Z. Wang and X. Liu, Role of electromagnetic interactions in the $X(3872)$ and its analogs, *Phys. Rev. D* **109**, 094002 (2024).
- [82] Y. R. Liu, M. Oka, M. Takizawa, X. Liu, W. Z. Deng and S. L. Zhu, $D\bar{D}$ production and their interactions, *Phys. Rev. D* **82**, 014011 (2010).
- [83] X. D. Yang, F. L. Wang, Z. W. Liu and X. Liu, Newly observed $X(4630)$: a new charmoniumlike molecule, *Eur. Phys. J. C* **81**, 807 (2021).
- [84] R. Q. Qian, F. L. Wang and X. Liu, Finding interaction mechanism between exotic molecule and conventional hadron, *Phys. Lett. B* **862**, 139329 (2025).
- [85] J. He and X. Liu, The open-charm radiative and pionic decays of molecular charmonium $Y(4274)$, *Eur. Phys. J. C* **72**, 1986 (2012).
- [86] M. B. Wise, Chiral perturbation theory for hadrons containing a heavy quark, *Phys. Rev. D* **45**, R2188 (1992).
- [87] R. Casalbuoni, A. Deandrea, N. Di Bartolomeo, R. Gatto, F. Feruglio, and G. Nardulli, Light vector resonances in the effective chiral Lagrangian for heavy mesons, *Phys. Lett. B* **292**, 371 (1992).
- [88] R. Casalbuoni, A. Deandrea, N. Di Bartolomeo, R. Gatto, F. Feruglio, and G. Nardulli, Phenomenology of heavy meson chiral Lagrangians, *Phys. Rep.* **281**, 145 (1997).
- [89] T. M. Yan, H. Y. Cheng, C. Y. Cheung, G. L. Lin, Y. C. Lin, and H. L. Yu, Heavy quark symmetry and chiral dynamics, *Phys. Rev. D* **46**, 1148 (1992).
- [90] F. L. Wang, R. Chen, Z. W. Liu and X. Liu, Possible triple-charm molecular pentaquarks from $\Xi_{cc} D_1 / \Xi_{cc} D_2^*$ interactions, *Phys. Rev. D* **99** no.5, 054021 (2019).
- [91] R. Machleidt, The High precision, charge dependent Bonn nucleon-nucleon potential (CD-Bonn), *Phys. Rev. C* **63**, 024001 (2001).
- [92] R. Machleidt, K. Holinde and C. Elster, The Bonn Meson Exchange Model for the Nucleon Nucleon Interaction, *Phys. Rept.* **149**, 1 (1987).

[93] X. Cao, B. S. Zou and H. S. Xu, Phenomenological analysis of the double pion production in nucleon-nucleon collisions up to

2.2 GeV, *Phys. Rev. C* **81**, 065201 (2010).